Electron Beam Induced Luminescence of Disordered SiO_2 Optical Coatings

JR Dennison[1], Amberly Evans[1], Gregory Wilson[1], Justin Dekany[1], Charles W. Bowers[2] and Robert Meloy[3]

[1]Materials Physics Group
Utah State University, Logan, UT 84332

[2]NASA Goddard Space Flight Center
Greenbelt, MD 20771

[3] MEI Technologies, Inc.
Greenbelt, MD 20771

Experimental Details

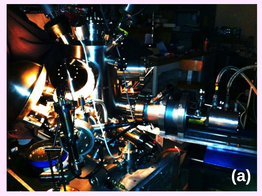

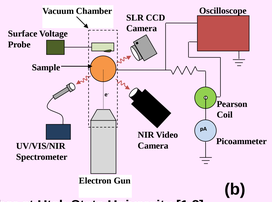

(b)

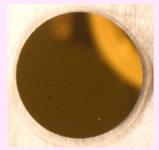

(c)

(a) UHV Electron Emission Test (EET) chamber at Utah State University [1,8].
(b) Block diagram of instrumentation for collecting the cathodoluminescence, data pulse charging surface voltage, and electrode current and induced by electron beam bombardment. Instrumentation includes: UV/Vis (200 nm to 1080 nm) and IR (900 nm to 1700 nm) fiber optic spectrometers, an SLR CCD still camera, an image intensified Vis/NIR video camera (400 nm to 900 nm), and a NIR (900 nm to 1700 nm) video camera for optical measurements and picoammeters, Pearson coils, and a storage oscilloscope for electrode current measurements [1].
(c) Samples (2.5 cm diameter) of optically smooth, thin film (~65 nm thick) disordered SiO_2 (fused silica) deposited on ~175 nm thick highly reflective, optically smooth metallic layers on a 2 mm thick fused quartz substrate.

Model of Cathodoluminescent Intensity

Luminescent Intensity Dependence on Beam Energy and Flux and on Material Optical Parameters

Luminescent intensity, I_γ, scales with incident current density J_b, beam energy E_b, temperature T, and photon wavelength λ as

$$I_\gamma(J_b, E_b, T, \lambda) \propto \dot{D}(J_b, E_b)\left[\frac{1}{\dot{D}+\dot{D}_{sat}}\left(\frac{\varepsilon_{ST}}{k_B T}\right)\right]\{\mathbb{A}_f(\lambda)[1+\mathbb{R}_m(\lambda)]\}$$

which is proportional to:

- Number of electrons in Shallow Traps (ST), thermalized from CB electrons
  - Trapping rates proportional to number of electrons excited in to CB which is proportional to dose rate
  - Retention rates leads to saturation at high charge, related to dose and T-dependant $\dot{D}_{sat}$ from RIC [5]
- Number of available Deep Trap states, dependant on space charge and T (see T-dependant discussion)
- Emitted photon absorption
  - Proportional to $\mathbb{A}_f(\lambda)$, the optical absorption coefficient of the coating
  - Enhanced by a factor $[1+\mathbb{R}_m(\lambda)]$, to account for reflection from the metallic layer

where the deposited power per unit mass (dose rate) is:

$$\dot{D}(J_b, E_b) = \frac{E_b\, J_b[1-\eta(E_b)]}{q_e \rho_m} \times \begin{cases} [1/L] & ; R(E_b) < L \ ; \ \text{non-penetrating radiation} \\ [1/R(E_b)] & ; R(E_b) > L \ ; \ \text{penetrating radiation} \end{cases}$$

which is proportional to incident electron absorption:

- Incident areal power density, $(J_b \cdot E_b)/q_e$
- Energy-dependant correction for unabsorbed quasielastic backscattered electrons, $[1-\eta(E_b)]$
- For biased samples, or when excess charge is stored in the trap states, a surface voltage V_s results and E_b is replaced everywhere by the landing energy, $[E_b - q_e \cdot V_s]$
- Absorbing mass, $m_{absorb} = \rho_m \cdot$ (Beam Area · Penetration Depth)
- Only a fraction of the incident power, $[L / R(E_b)]$, when range exceeds sample thickness

Luminescent Intensity Dependence on Thickness and Range

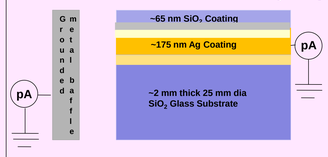

(Left) Layered cross section of disordered SiO_2 and Ag sample. (Lower Left) Range and dose rate of disordered SiO_2 as a function of incident energy using calculation methods and the continuous slow-down approximation described in [9]. (Lower Right) Dose rate as a function of incident energy in each layer of multilayer sample, assuming a flux density of 10 nA/cm² and beam area of 4.9 cm² [9].

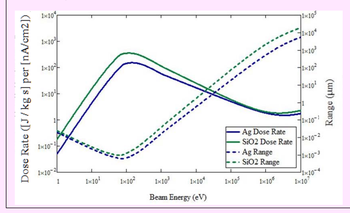

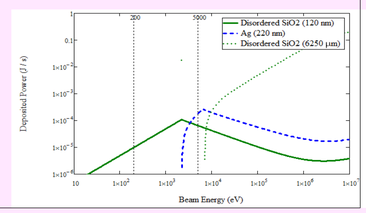

Acknowledgements and References

Funding for this project was from NASA Goddard Space Flight Center and an NASA NATRF Fellowship.

[1] A. Evans, G. Wilson, J. Dekany, A.M. Sim and JR Dennison "Low Temperature Cathodoluminescence of Space Observatory Materials," Proc. 12th Spacecraft Charging Techn. Conf., (Kitakyushu, Japan, 2012).
[2] V. Grisen, L.A. Dissado, J.C. Fothergill, C. Laurent and G. Teyssedre, "Photoluminescence, recombination induced luminescence and electroluminescence in epoxy resin," J. Phys. D: Appl. Phys, vol. 34, pp. 2534-2540, 2001.
[4] A. Joblonski,Über den Mechanismmus des Photoluminescence voFarbstoff - phosphoren," Z. Phys., Vol. 94, pp.38-46, 1935.
[5] J.R. Lakowicz Principles of Fluorescence Spectroscopy, Plenum Press, New York, 1983.
[6] R. Salh, A. von Czarnowski, M.V. Zamoryanskaya, E.V. Kolesnikova and H.-J. Fitting, "Cathodoluminescence of SiO_x Under-stoichiometric Silica Layers," Phys. Stat. Sol., vol. 203, pp. 2049-2057, Apr. 2006.
[7] A.N. Trukhin, M. Goldberg, J. Jansons, H.-J. Fitting and I.A. Tale, "Silicon Dioxide Thin Film Luminescence in Comparison with Bulk Silica," J. Non-Crystalline Sol., 223,114, 1998.
[8] G. Wilson, JR Dennison, A. Evans and J. Dekany "Electron Energy Dependent Charging Effects of Multilayered Dielectric Materials" Proc. 12th Spacecraft Charging Techn. Conf., (Kitakyushu, Japan, 2012a).
[9] G. Wilson and JR Dennison, "Approximation of Range in Materials as a Function of Incident Electron Energy," IEEE Transaction on Plasma Science, IEEE Trans. on Plasma Sci., 40(2), 305-310 (2012b).

Abstract

Optical coatings of disordered thin film SiO2/SiOx dielectric samples on reflective metal substrates exhibited cathodoluminescence under electron beam irradiation. Measurements of the absolute radiance and emission spectra as functions of incident electron energy, flux and power over a range of sample temperatures are reported. Radiance reached a saturation plateau at high incident electron power. Well below saturation radiance scaled with deposited power, that is linearly with incident power for lower-energy non-penetrating electrons and decreasing with increasing energy for penetrating radiation. Four bands were observed in spectral measurements from 300 nm to 1000 nm. Changes in peak intensity and shifts in peak energies as functions of temperature are described. The observations are explained in terms of a simple disordered band theory model and the transitions that take place between electrons in extended conduction states and localized trapped states associated with structural or compositional defects in the highly disordered insulating materials; this provides a fundamental basis for understanding the dependence of cathodoluminescence on irradiation time, incident flux and energy, and sample thickness and temperature.

Disordered Bandstructure Model

Bandstructure Determines Conductivity. Disorder Introduces Localized Defect States in Band Gap

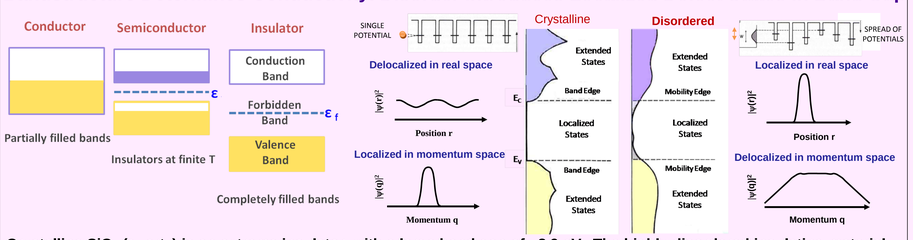

Crystalline SiO_2 (quartz) is an extreme insulator, with a large band gap of ~8.9 eV. The highly disordered insulating material, disordered SiO_2/SiO_x, has additional localized trap states within the band gap, resulting from structural and substitutional disorder. These act to enhance the conductivity, by providing partially filled states within a few k_BT of the CB edge.

Defect Type Determines Deep Trap Energy

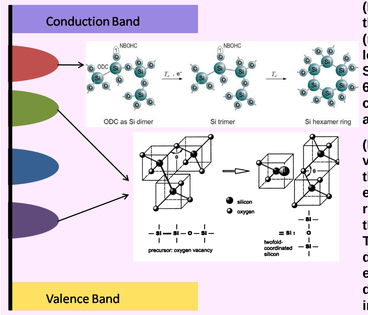

Transitions to Defect States Determine Wavelengths

(Left) The existence of at least four peaks in the disordered SiO_2 luminescence spectra (right) suggest at least four bands of localized defect or "deep trap" (DT) states. SiO_2 studies at room-T have attributed a 645 nm peak to a nonbridging oxygen hole center [6] and 275 nm and 500 nm peaks to an oxygen deficient center [7].

(Right) Mofdified Joblonskidiagram [4] of valence band (VB) electrons are excited into the conduction band (CB) by the high energy incident electron radiation. They relax into shallow trap (ST) states, then thermalize into lower available long-lived ST. Three paths are possible: (i) relax-ation to deep traps (DT), with concomitant photon emission; (ii) radiation induced con-ductivity (RIC), with thermal re-excitation into the CB; or (iii) non-radiative transitions or e⁻-h⁺ recombination into VB holes.

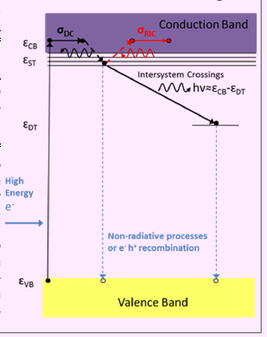

Deep Trap Occupation Determines T-Dependence

We began with a simple two band model to qualitatively explain the T-dependence of observed spectra [1].

- The Fermi energy of a material is the energy of the highest filled state at T=0 K.
- The Fermi level, E_F, is the (weakly) temperature dependant chemical potential defined as the energy for 50% probability filling a state.
- The effective Fermi level, E_F^{eff} can be thought of as a charge- and T-dependant chemical potential, resulting from inject of additional charges.

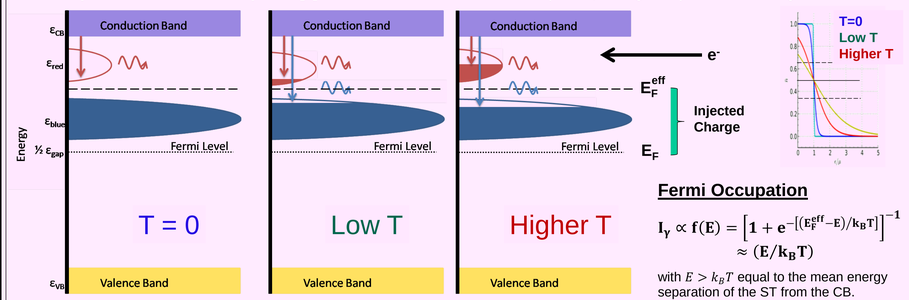

Fermi Occupation

$$I_\gamma \propto f(E) = \left[1 + e^{-[(E_F^{eff}-E)/k_BT]}\right]^{-1} \approx (E/k_BT)$$

with $E > k_BT$ equal to the mean energy separation of the ST from the CB.

At T=0 stored charge from the beam fills all trap states below an effective Fermi level. Thus, only the higher (red) band has unoccupied states to transition into and emit photons.

At low T with $0<k_BT<<(\varepsilon_{red}-\varepsilon_{blue})$, a significant number of electrons in the blue band are thermally excited to the red band. This creates available states in the blue band, so blue photons can be generated.

At higher T with $0<<k_BT<(\varepsilon_{red}-\varepsilon_{blue})$, even more electrons from the blue band are thermally excited into the red band, creating more available blue trap states and blue photons.

Measured Results

SLR CCD Camera Data

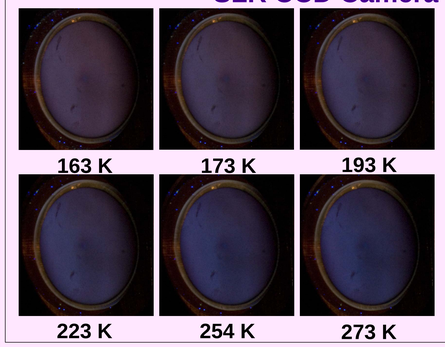

SLR CCD camera images showing temperature dependency of SiO_2 cathodoluminescence:

- At low T, glow appears both red and blue.
- As the sample T increases from 163 K to 273 K, the red light becomes much less intense and the glow appears to be dominantly blue.

Plotting Red-Green-Blue (RGB) component intensities of SLR images vs T, we find red intensity decreases and blue intensity increased with increasing T.

UV/Vis/NIR Spectral Data

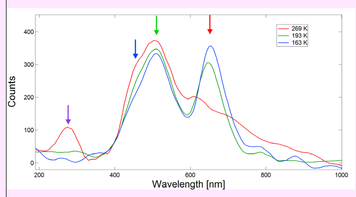

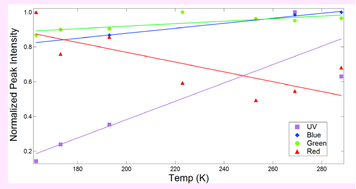

(Left) Three luminescence UV/VIS spectra at decreasing sample temperature. Four peaks are identified: red (~645 nm), green (~500 nm), blue (~455 nm) and UV (275 nm) with FWHM ~80 meV.

(Right) Peak amplitudes of four peaks as a function of sample temperature, with baseline subtracted and normalized to maximum amplitudes. This verified the T-dependent behavior observed in the SLR images.

Luminescent Intensity Data

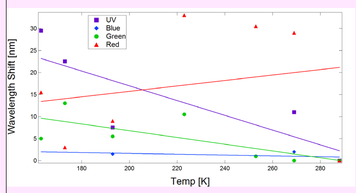

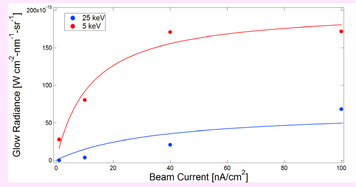

(Left) Peak wavelength shift as a function of sample temperature. Red peak shifts to low wavelength with increasing T; all other peak shift in the opposite direction. This is consistent with an effective Fermi level below the red peak, as explained in the T-Dependence panel at left.

(Right) Total luminescent radiance vs beam current at fixed incident energy. Saturation effects are evident at higher currents. Data are consistent with fits shown, based on the master intensity equation at left.

Luminescent Intensity Energy Dependant Data

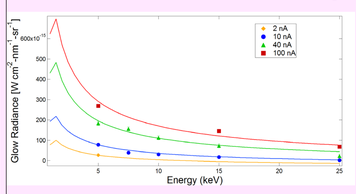

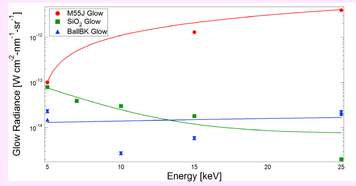

(Left) Total luminescent radiance versus beam energy at fixed incident flux fit by the master intensity equation at left.

(Right) Total luminescent radiance vs beam energy at fixed 10 nA/cm² incident flux for:
(red) Epoxy-resin M55J carbon composite. A linear fit works, since the thickness of epoxy exceeds the penetration depth of 25 keV electrons,
(green) SiO_2 coated mirror; fit with decreasing master intensity equation as seen in Left figure,
(blue) Carbon-loaded polyimide black Kapton 230XC275 (triangles for 10 nA/cm² and hour glasses for 30 nA/cm² linearly scaled to 10 nA/cm²). Intensity is almost independent of energy. Perhaps the highly absorptive carbon particles limits the thickness that allow photon emission.